Mechanical Systems and Signal Processing 172 (2022) 108914

Contents lists available at ScienceDirect

Mechanical Systems and Signal Processing

journal homepage: www.elsevier.com/locate/ymssp

Failure diagnosis system using a new nonlinear mapping augmentation approach for deep learning algorithm

Dong-Yoon Kim [a], Yeon-Jun Woo [a], Keonwook Kang [b,*], Gil Ho Yoon [a,**]

[a] School of Mechanical Engineering, Hanyang University, Seoul, South Korea
[b] School of Mechanical Engineering, Yonsei University, Seoul, South Korea

ARTICLE INFO

Communicated by D. Nikolaos

Keywords:
Transverse vibration
Damage
Frequency response function
Virtual spectrogram
Nonlinear mapping
Data augmentation

ABSTRACT

This paper develops a new nonlinear transformation-based augmentation method for Convolutional Neural Network (CNN) approach with vibration signals of simple, small scale and elementary reference models for the classification or prediction of vibration signals of perplex healthy or damaged systems using a smart diagnosis system. The accuracy of deep learning algorithm being highly dependent on the quantity of qualified data, the acquiring of a large set of formatted data for the training and verification of a deep learning algorithm is essential. Unfortunately, many scientific and engineering application domains do not allow access to a Big Data accurately bearing domain knowledge and the artificial intelligent (AI) based classification methods suffer from the lack of data and often end up with poor prediction. To overcome this issue, data augmentation approaches have been utilized. In many applications, however, the obtaining of data reflecting physical phenomena is even not possible. To overcome this issue, this research suggests a new nonlinear transformation-based augmentation approach mapping from the data obtained from lab-scale healthy models to the data of complex real healthy models whose data in the damaged status are hard to be obtained. The nonlinear transformation method defined between the data of lab-scale healthy models and the data of complex real healthy model is then applied to predict the data of complex real damaged models for an accurate classification. To validate the concept of the nonlinear transformation augmentation, several vibration examples including an example showing the mode switching are considered. To extract discriminating features from the vibration-based spectrograms using a deep learning algorithm, the nonlinear transformation-based augmentation and the classification between healthy and damaged structures are presented.

1. Introduction

This paper develops a new nonlinear transformation-based augmentation method of vibration signals of simple, small scale and elementary models for Convolutional Neural Network (CNN) approach for the classification and prediction of perplex healthy or damaged systems using a smart diagnosis system. As the accuracy of a deep learning algorithm is dependent on the number of training data, the acquiring of a large set of data for the training and verification of the deep learning is essential. Unfortunately, many engineering application domains do not allow access to big data reflecting domain knowledge or suffer from the lack of data and often end up with poor prediction. To overcome this issue, the data augmentation approaches have been utilized to increase the

* Corresponding author at: School of Mechanical Engineering, Yonsei University, Seoul, South Korea.
** Corresponding author at: School of Mechanical Engineering, Hanyang University, Seoul, South Korea.
E-mail addresses: kwkang75@yonsei.ac.kr (K. Kang), ghy@hanyang.ac.kr (G.H. Yoon).

https://doi.org/10.1016/j.ymssp.2022.108914
Received 27 June 2021; Received in revised form 30 November 2021; Accepted 28 January 2022
Available online 5 March 2022

Table 1
Simplified and complex models for the nonlinear transformation function.

	Experiment	
	Healthy condition	Damaged condition
Reference model	Easy	Difficult
Complex real model	Easy	Difficult or impossible

size and quality of data [1–4]. These data augmentation approaches still require some big data. In addition, the obtaining of data reflecting physical phenomena is even not possible in many applications. To address this impossibility and difficulty, this research develops the nonlinear transformation based augmentation approach mapping from the data of lab-scale reference healthy models to the data of complex real healthy models whose data in damaged status are hard to be obtained (see Table 1). The nonlinear transformation function between the lab-scale reference healthy models and the complex real healthy model is then applied to the complex real damaged models for the data augmentation of the deep learning. In order to extract discriminating features from the vibration-based spectrograms, the nonlinear transformation based augmentation and the classification between healthy and damaged structures are presented.

Recently, a lot of research have been conducted on methods of detecting an abnormality in structure by measuring vibration signals using deep learning. In some applications, a method of classifying delamination of composite materials using vibration signals through deep learning was employed [5,6]. Fault diagnosis of the complex system was performed with frequency response function using a CNN-based deep learning algorithm [7]. A new deep learning model has been also proposed to deal with the fault diagnosis problem using raw vibration signals [8]. Although an augmentation method has been proposed, it is not easy to obtain data which reflect physical phenomena such as airplane, building, and human. A technology for predicting the results by computer simulation of a real model called digital twins has been researched [9]. In addition, a method of diagnosing machinery faults using a digital twin was also carried out [10,11]. In [12], the deep learning based diagnostic procedure was developed for the identification of engine defects of 2-wheeler vehicle. A procedure detecting the working condition of a three-phase induction motor was proposed in [13]. In [14], a fault diagnosis method was developed to identify bearing faults such as multi-scale cracks and high shaft speed vibrations using CNN. A review of the applications of the deep learning algorithm toward structural building damage detection was given in [15]. The detection of the location within a building with smart building vibration based sensors was investigated in [16]. To diagnose the faults, a new fault diagnosis methods are studied [17–19].

In addition, to generate an optimal mesh, automatically fine-tunes is studied with exponential convergence of numerical errors to mesh size in [20]. The cyber physical production system based on FEM is presented for a digital twin that combines simulation and machine learning in [21]. The new nonlinear transformation and the simple peak finding strategy were studied to detect the automatic R-wave in [22]. Some nonlinear signal transforms were developed about the slope content of signals and are useful for analytic tools of nonlinear systems in [23]. To provide the basic concepts of the scaling and dimensional analyses, the modeling of the instrumented indentation was considered [24]. An application method of the dimensional analysis and scaling was presented [25]. A transfer learning method that generates high-performance learners trained with more easily obtainable data in different domains is studied [26,27]. To solve brittle fracture problems, the retrain method of network partially while keeping the weights and the biases using transfer learning is considered [28].

Data augmentation encompasses a suite of techniques that enhance the size and quality of training dataset such that a better deep learning models can be built utilizing them. This study develops a new transformation-based augmentation method in Fig. 1 to solve the issue to enhance the size and quality of training dataset for a better deep learning model. The data augmentation method is one of the key components in deep learning algorithm to enlarge the dataset and it is based on a limited number of data. However, in some applications, acquiring data is impossible. To overcome this, a new transformation-based augmentation method shown in Fig. 1 is presented here. The method carries out the nonlinear transformation mapping from the data of simplified lab-scale healthy reference models to the data of complex real healthy model. The nonlinear transformation function between the responses of the lab-scale reference healthy models and the complex real healthy model is then applied to predict the responses of the complex real damaged models for the data augmentation of the deep learning. To obtain discriminating features from the vibration-based spectrograms, the nonlinear transformation and the classification between healthy and damaged structures are proposed.

The paper is organized as follows. Section 2 develops the nonlinear mapping function and explains its concept to augment data. In Section 3, the applications of the deep learning algorithm are incorporated with the present nonlinear mapping function. In Section 4, several examples of the nonlinear mapping function are presented. The responses of undamaged and damaged simplified reference models are transformed and their responses are compared. The signals of damaged reference models are mapped with the nonlinear mapping function to mimic the signals of damaged real model. Then, the virtual spectrogram images are generated for the deep learning algorithm. Section 5 provides the conclusions and suggestions for future research topics.

2. Data augmentation with the nonlinear transformation function

2.1. Simplified reference model and complex real model

This section develops the nonlinear transformation function mapping the low-frequency response functions of simplified reference models and complex real models whose analysis and experiments are often perplex; particularly it is assumed that the responses of

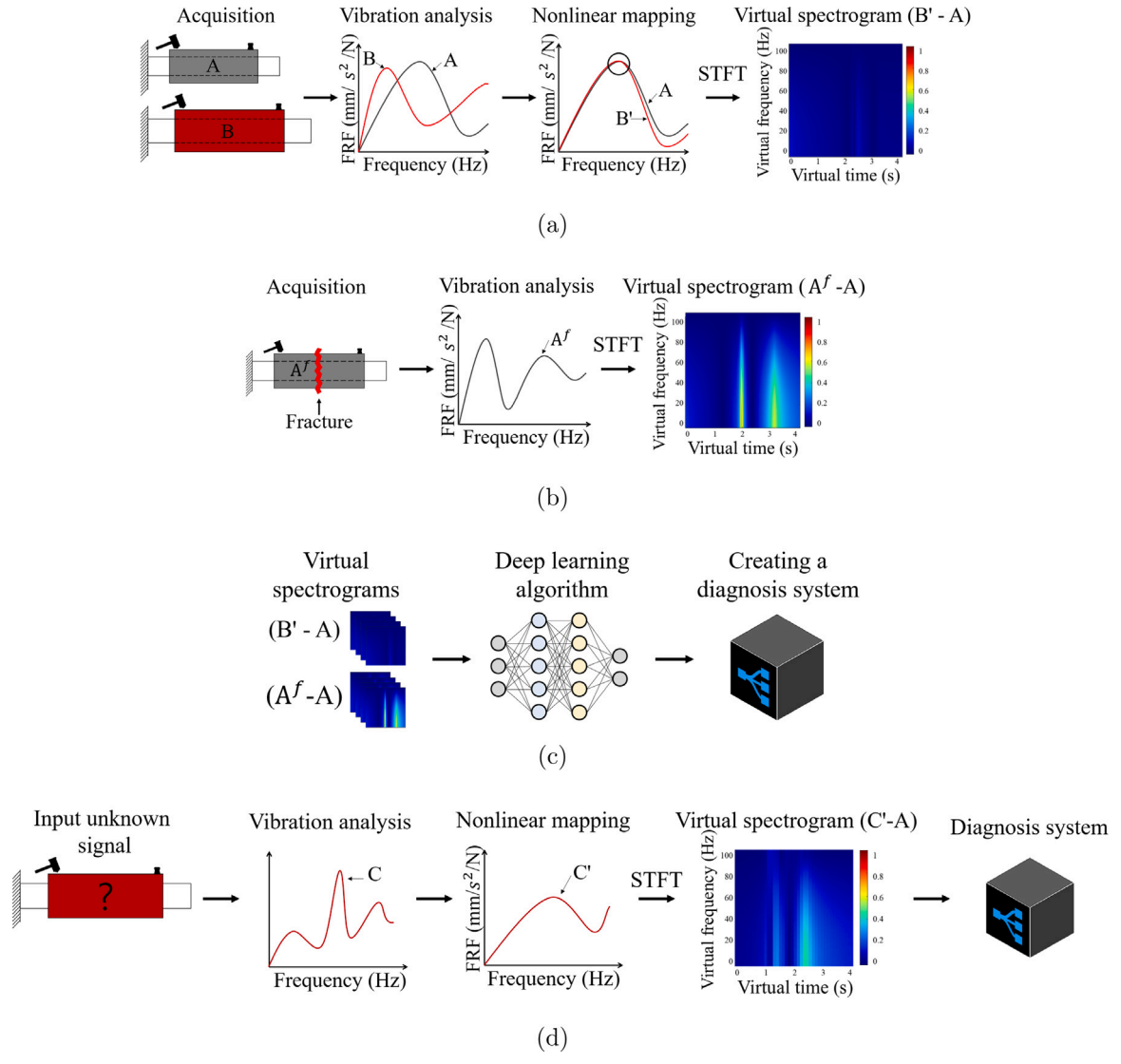

Fig. 1. Procedure of the fault diagnosis system. (a) The definition of the nonlinear transformation function using the vibration signals with healthy models (A: healthy reference model, B: healthy real model), (b) the virtual spectrogram with the vibration data of the damaged reference model, (c) the process of creating diagnosis system using a deep learning algorithm with virtual spectrograms, and (d) the determination of damage using the diagnosis system with the virtual spectrograms of a mapped unknown signal.

damaged real system is impossible. The overall procedure developed here is outlined in Fig. 1. The simplified reference models refer lab-scaled models to easily evaluate their responses with different materials, boundary conditions and various factors determining responses. They can be geometrically scaled models for mega structures or can be cheap and disposable models substituting expensive or delicated models. Compared with complex real models, a serious issue to carry out experiments with or without damage does not exist for the simplified reference model. However, they should reflect some important aspects of complex real models that are used to identify the physical responses of complex real systems. Inevitably some differences exist between simplified reference models and complex real models and the applications of data augmentations inevitably are limited. To overcome this aspect and difficulty, the nonlinear transformation function is presented here. It is assumed that the experiments of real system with damages are difficult and sometimes impossible as follows:

- Assumption 1: The dynamic responses of the ***healthy*** and ***damaged*** simplified reference models are easily obtained.
- Assumption 2: The responses of complex real ***healthy*** models are easily obtained.
- Assumption 3: The responses of complex real ***damaged*** models are difficult to obtain and often are not available.

- Assumption 4: Despite the differences between simplified reference models and complex real models, the orders of the mode-shapes and the associated frequency values are similar. Indeed, an approximate nonlinear transformation function scaling the frequency axes and the responses between the two models can be defined. Note that the characteristics such as size, material properties and the location of crack of simplified reference models have not to be same with those of complex real models.

To develop the nonlinear transformation function, the above things are assumed. The first assumption states the necessity of the simplified reference model. For example, the vibration data of a real-scale building can be easily obtained in healthy condition and measured. However, it is a non-sense to destruct mega structure or building to obtain the vibration data only for the healthy monitoring comparing vibration data. It is possible to collect the responses of old buildings or after several decades but it is not intended in this research. This kind of situation can be found in various scientific and engineering applications such as airplane, building, ship, aeronautics or human health monitoring. Thus, this research adopts the second and third assumptions. The fourth assumption means that it is possible to make a small scale reference model with and without damage easily to collect vibration data for monitoring. In addition, it is assumed that the mode shapes of the small scale reference model are similar to those of the complex real model of interest. If the order of the modes is subject to be changed, the order of the modes must be adjusted accordingly. Thus, the response frequency values are different but the orders of the eigenmodes are similar or can be matched together. The remaining issue is then how to generate the vibration data of damaged real system. This research intends to find out the approximately response of the damaged complex real model by defining the nonlinear transformation function between the responses of the healthy simplified reference model and the healthy complex real model.

The frequency response functions of finite element models with and without damage are compared and analyzed. The benefit of the finite element models lies in the facts that it is easy to change the boundary conditions including the size and location of damage and the repeatable results can be obtained.

2.2. The nonlinear transformation function

This subsection presents the nonlinear transformation with a healthy simplified model and a healthy complex real model. The transformation function defined here is then applied to unknown signals to determine the existence of damage or fracture. To match a healthy signal of real model to a healthy reference signal of simplified model in the FRF (Frequency Response Function), the nonlinear transformation should be defined. This function matches the resonance frequencies of the healthy reference system to the resonance frequencies of the healthy system. In addition, it is aimed that the slopes are matched together through the function. Without the loss of generality, the following FRF is assumed.

$$Y = H(\omega) \tag{1}$$

where the frequency response and its response function are denoted by Y and H, respectively. The angular velocity is denoted by ω. First of all, the peak frequencies and amplitudes between simplified reference models and complex real models are matched by shifting angular speed and shifting and scaling of amplitude.

$$\text{Shifting of angular speed}: \tilde{\omega_c} = \left(\frac{H_s^{-1}(Y_{max}^s)}{H_c^{-1}(Y_{max}^c)} \right) \cdot \omega_c \tag{2}$$

$$\text{Shifting and scaling of amplitude}: \tilde{Y_c} = \left(\frac{Y_{max}^s - Y_{min}^s}{Y_{max}^c - Y_{min}^c} \right) \cdot Y_c \tag{3}$$

where the frequency response and the transfer function of real system are denoted by Y_c and H_c, respectively. Those of simplified reference model are denoted by Y_s and H_s, respectively. The maximum FRF values of simplified reference model and complex real model are denoted by Y_{max}^s and Y_{max}^c, respectively. The minimum FRF values of each model are denoted by Y_{min}^s and Y_{min}^c, respectively. The resonance frequencies of healthy signal of complex real model is denoted by ω_c.

With the above nonlinear mapping scheme, the frequency responses of the *healthy* simplified reference model and the *healthy* complex real model are approximately matched and scaled together. The defined nonlinear transformation function is now able to map the response function of the damaged simplified reference model to predict the response of damaged real model. Note that this research assumes that the transferred response function of the damaged simplified reference model shows the similar response of the damaged complex real model. Thus, it is possible to augment the data which are necessary in a smart diagnosis system. In short, the responses of *healthy* simplified reference model and complex real model are defining the nonlinear transformation function which can also transfer the responses of *damaged* complex real model to the approximate responses of *damaged* simplified reference model.

To use the present nonlinear transformation function in the framework of the present smart diagnosis system, the following procedures are carried out successively. The responses are named and defined as follows:

- H.R.S. : Healthy Reference Signal
- D.R.S. : Damaged Reference Signal
- H.S. : Healthy Signal of complex real model
- M.H.S. : Mapped healthy signal with the present nonlinear transformation method

Step 1: Nonlinear transformation Function (H.S. ⇒ H.R.S.)

Define the nonlinear transformation function by mapping the H.S. response to the H.R.S response. With the nonlinear transformation function, the M.H.S. can be plotted and the similarity between the M.H.S. and the H.R.S. response can be observed for the frequency domain of interest.

Step 2: Signal mapping of unknown real system (U.S. ⇒ M.U.S.)

For the next step, a real system whose condition is not known is measured. The measured response is set to the U.S. signal. In the present study, the U.S. signal is the transverse vibration. When the signal is sufficiently similar to the signal of the H.S., it is not necessary to procedure further. However, in case of some differences, the nonlinear transformation function can be used to map the U.S. signal to the M.U.S. whose responses are assumed to be similar to the responses with the reference model with the similar damages of the reference model. With this nonlinear transformation function, therefore, it is possible to compare the M.U.S. and the D.R.S..

2.3. Determination of healthy or damage case

The defined transformation can predict the signals of damaged real systems by transforming the responses of damaged reference model. Note that the function is defined in the bases of the responses of healthy simplified and complex real models. Thus, the following measure and determination of the existence of damage can be possible.

$$\begin{cases} \text{Healthy case if } Y_s \approx \tilde{Y}_c \\ \text{Damage case if } Y_s \neq \tilde{Y}_c \end{cases} \tag{4}$$

If the difference between the healthy reference signal of the simplified reference model and the mapped healthy signal of the complex real model by the nonlinear transformation function is small and is small enough, the real model is defined as healthy condition. This is due to that the response curves of the simplified healthy reference model and the mapped healthy signal become close to each other and the difference becomes small enough. However, if there is a damage to a complex real model, the difference will be large in (4). The flowchart of the entire nonlinear mapping process is presented in Fig. 2. For the rigorous determination and classification using the procedure, a deep learning algorithm can be incorporated. To achieve this, the virtual spectrogram interpreting the frequency as the virtual time and the difference of the frequency response functions as the signal is employed for the deep learning algorithm in the next section.

2.4. Mode switching with an empirical function

This subsection presents a method to adjust the amplitude in case the mode crossing phenomenon occurs. With the mode switching phenomenon, this research proposes the reordering process of the frequency response function. The reordering step is performed by switching the crossed modes of the real complex model in the order of the modes of the reference model. To achieve this, the frequency response function is divided at the middle points among the resonance peaks. Then, the divided FRF curves are reordered, shifted and scaled. To adjust the dissected curve smoothly, the following empirical process is performed.

$$\tilde{Y}_n = \begin{cases} Y_n, & n = 1 \\ Y_n - (Y_n^f - Y_{n-1}^l), & n \geq 2 \end{cases} \tag{5}$$

where the last amplitude of the previous section of FRF is denoted by Y_{n-1}^l and the first amplitude value of the next section is denoted by Y_n^f. The next section of the FRF and the adjusted section of FRF are denoted by Y_n and $\tilde{Y}_n$. With the above formulation, the FRF with the mode crossing phenomena is reordered and shifted to be a smooth curve.

3. Deep learning algorithm for damage detection with the nonlinear transformation function

This section presents the application of the CNN trained with the virtual spectrograms of structural vibration responses mapped with the nonlinear transformation function in (2) and (3).

3.1. Application of CNN (Convolutional Neural Network)

The CNN becomes a very effective image classification tool for various scientific and engineering applications [29–38]. One of the key requirements of the CNN algorithm is the collection of image data containing and featuring physical significance. Some typical operations of the CNN are Convolution operator, Rectified Linear Unit (ReLU) substituting the Sigmoid function, Pooling or Subsampling, and classification. The conventional CNN is composed of Convolution layer, Pooling layer or Subsampling layer, and Fully-connected layer [39–41]. The convolution layer is to extract discriminating features from training images to fit a problem

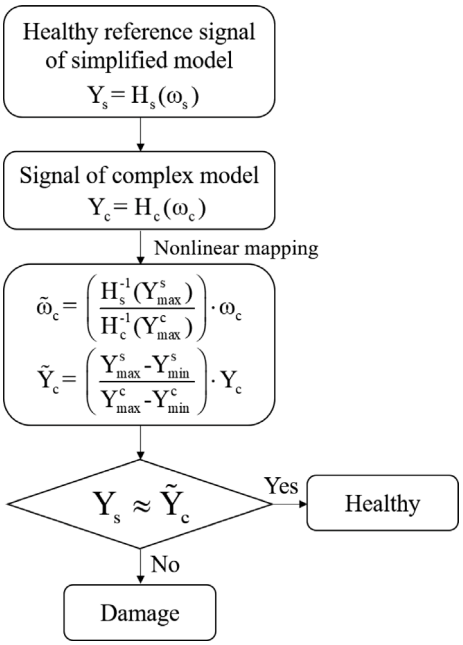

Fig. 2. Determination process based on the nonlinear mapping. (With the help of the virtual spectrogram, a deep learning algorithm can be incorporated.)

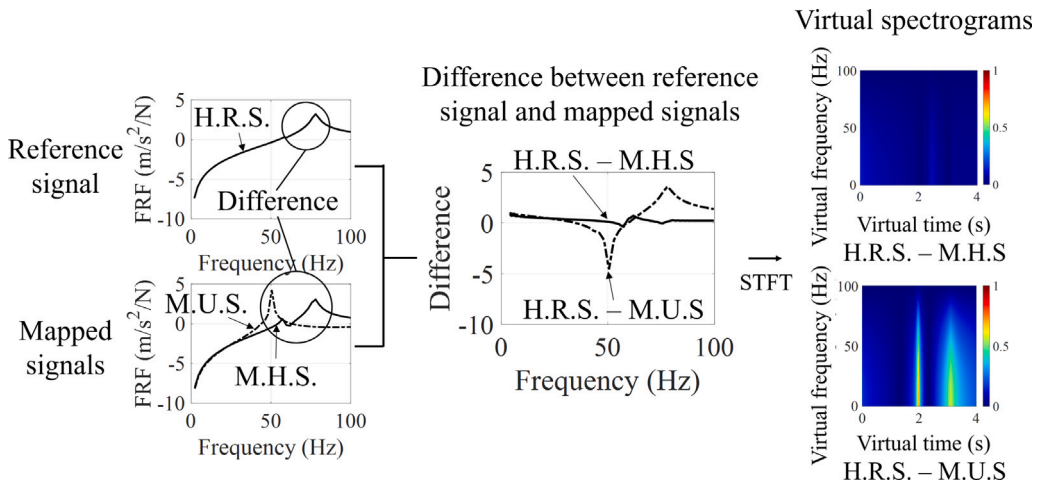

Fig. 3. Concept of the present virtual spectrograms interpreting the frequency as the virtual time and the differences as the signals.

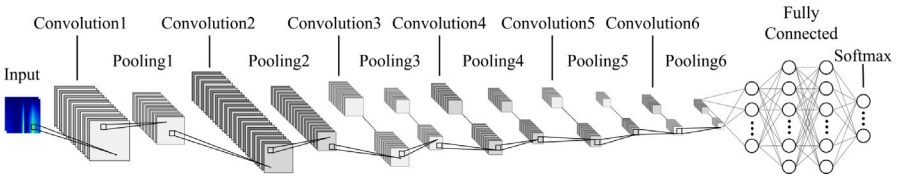

Fig. 4. CNN architecture.

of interest using filter or kernel. The convolutional layer applies the trained filter for input images to obtain feature maps and summarizes the features of the input images and the convolution layer is followed by a nonlinear operation (ReLU) [42]. The step called pooling or subsampling is applied in order to obtained downsampled data. The pooling layers transform the input images into a high-level feature maps. The mathematical details of CNN can be found in [43].

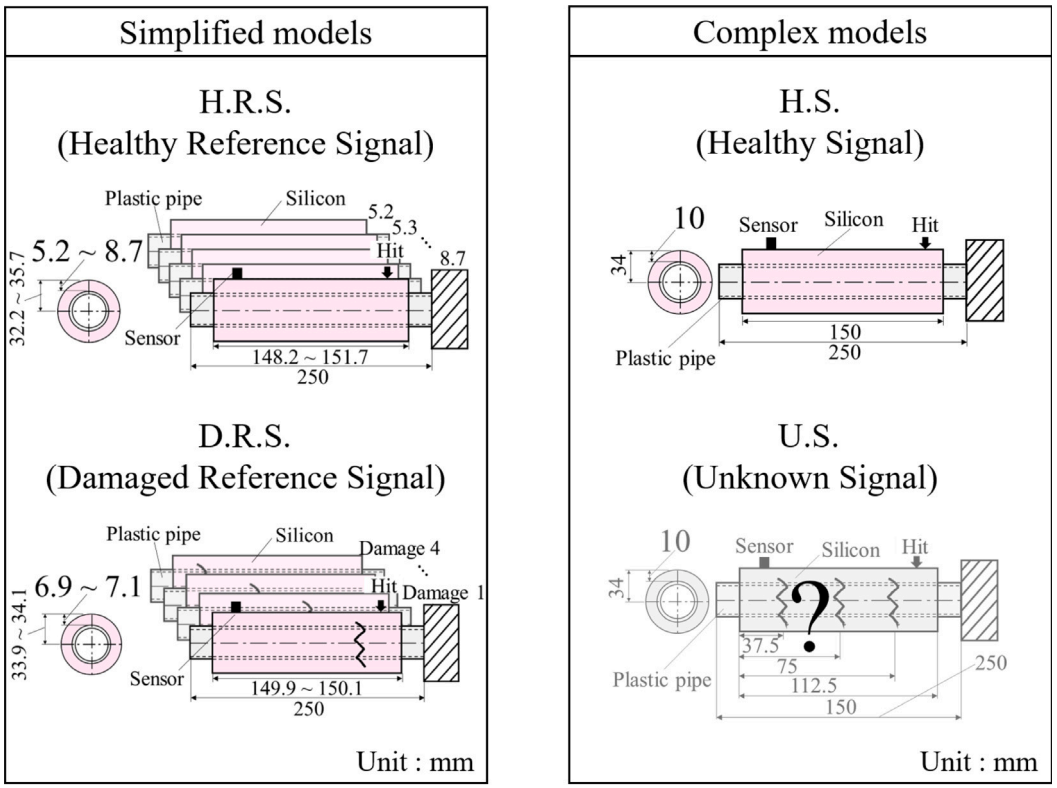

(a)

Fig. 5. Illustration of geometric configurations represented by simplified and complex models with plastic bar and silicon (silicon: $\rho = 1500\ \mathrm{kg/m^3}, \mathrm{E} = 1\ \mathrm{MPa}, \nu = 0.47$, plastic pipe: $\rho = 1330\ \mathrm{kg/m^3}, \mathrm{E} = 2\ \mathrm{GPa}, \ \nu = 0.4$).

3.2. Virtual spectrogram application

The presented virtual spectrogram was introduced in order to identify the existence of damage with the CNN algorithm [44]. The conventional spectrogram means two-dimensional visual representation of the frequency spectrum analyzed by the Short Time Fourier Transform (STFT). Unlike the conventional spectrogram, this research obtains the two-dimensional virtual spectrogram images analyzing the difference of the frequency response functions with the STFT as shown in Fig. 3. For this purpose, the transverse vibration data are obtained from the simplified reference models with/without damage and healthy complex real models. It is worth to notice that the data of *damaged* complex real model is not used to train the CNN. The nonlinear transformation function is defined with the transverse vibration data of the simplified healthy reference model and the healthy complex real models. This nonlinear transformation function in (2) and (3) is applied in order to augment the images data from *healthy* complex real model and *healthy/damaged* simplified models. The inverse of the nonlinear transformation function can be used to predict the responses of *damaged* complex real model using the responses of *damaged* simplified reference model. In other words, the responses of the various damaged simplified reference models can be transferred for those of the corresponding *damaged* complex real models. Through the nonlinear transformation function transferring the responses of the *healthy* complex real system to the responses of the *healthy* simplified reference model, the response of unknown real specimen can be found from the vibration data of the simplified reference model. If the differences of the responses of the unknown real specimen mapped with the present nonlinear transformation function and the *healthy* simplified reference model are large, it can be classified as the signals of the *damaged* real specimen. If not, it can be classified as the *healthy* specimen as illustrated in Fig. 1. In the present study, a set of the images of the two cases (healthy or damaged cases) were generated as shown in Fig. 3 and are used as the training data for CNN. Although it may be possible to employ another method, i.e., the wavelet transformation, the STFT method is successful to train the CNN.

3.3. CNN architecture

The CNN is trained for the classification approach with the virtual spectrogram images. Fig. 4 shows that the network consists of six convolutional and pooling layers for extracting discriminative features from the virtual spectrograms of the healthy and damaged cases. Fully connected layer are employed to classify the healthy and damaged cases on the basis of features extracted in

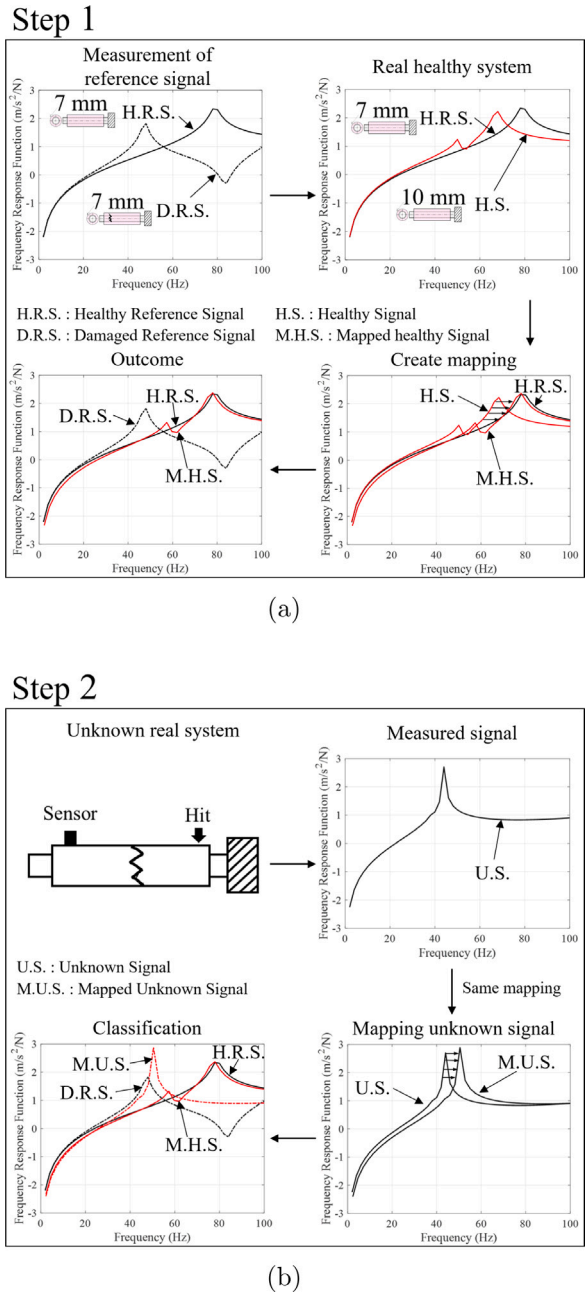

Fig. 6. The process of nonlinear mapping with plastic bar and silicon models. (a) Mapping process of reference signals of simplified models and healthy signal of complex model and (b) mapping process of reference signals of simplified models and unknown signal of complex models.

the convolutional and pooling layers. The architecture of this convolutional neural network is presented in detail in Table 2. The models are trained with a mini-batch size of 2 which means that the training data is divided into 2 sets, a set of random weights, the learning rate of 0.0001, and 20 epochs using the CNN implemented in MATLAB [45]. The CNN architecture was proposed to classify the virtual spectrograms of the 2 classes (healthy and damaged cases).

4. Application of the present nonlinear transformation function and the deep learning algorithm

To illustrate the application of the CNN based classification incorporating with the present nonlinear transformation function, this section presents three damage classification examples. With the vibration data and the frequency response functions from simplified reference model and healthy real model, the nonlinear transformation function is defined. The nonlinear transformation method can

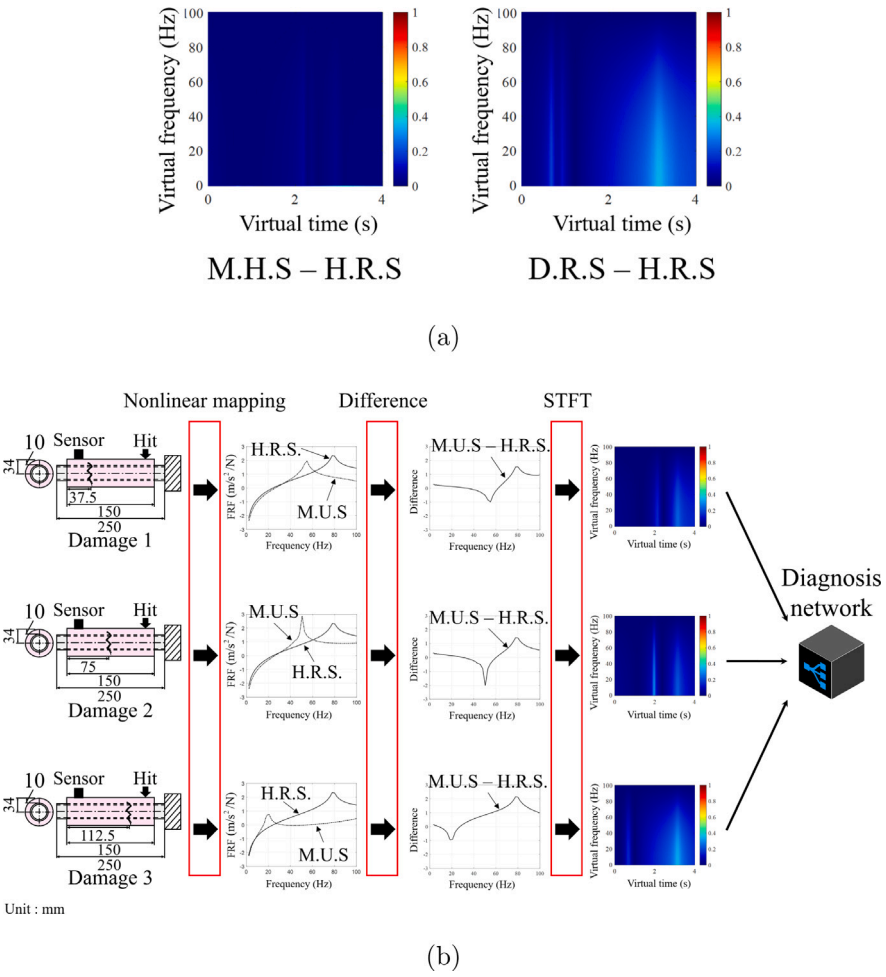

Fig. 7. The virtual spectrograms of the three different damages (the locations of the damages at 37.5 mm, 75 mm and 112.5 mm). (a) The virtual spectrograms with and without the damage and (b) the virtual spectrogram images of various damages.

roughly find out the frequency response function signals but cannot determine what condition it is by itself. To resolve this issue, we calculated the difference of the transformed frequency response function signals and the reference signals. Then, the images of the virtual spectrogram using the STFT method are obtained. To systematically determine health and damage condition, the CNN with virtual spectrogram images can be employed. Using the vibration data with the *healthy and damaged reference* models and the *healthy real* model, the training data are generated for the deep learning algorithm. The vibration data from the *damaged complex real* model are inserted to determine whether a model is damaged or not. The confusion matrices are presented to show the accuracy. The three models are considered, the straight plastic bar and silicon model is considered for the first example. The second example is the application of the present approach for bent plastic bar and silicon composite model. The third example is an example with the mode switching phenomenon. The mode switching phenomenon refers that the orders of the eigenmodes of simplified reference model and complex real model are switched [46,47].

4.1. Example 1: Plastic bar and silicon model

For a first example, the prediction of damage of plastic bar coated with silicon is considered in Fig. 5. The present study suggests utilizing plastic bar and silicon as they are easy to obtain and carry out experiments. In addition, their material properties are well known. To show the applicability of the present nonlinear transformation function, the finite element method is employed to obtain the frequency response functions of the simplified healthy/damaged models and the healthy/damaged complex real models. In the left column in Fig. 5, the simplified reference models without and with damage are presented. The vertical damages occurred in several places in the reference model were considered. It is assumed that the simplified reference models can be easily experimented and their responses can be easily obtainable. Without the loss of generality, the transverse vibration signals obtained at a sensor on the silicon crust are compared and analyzed (single input and single output). In the right column in Fig. 5, the complex real healthy

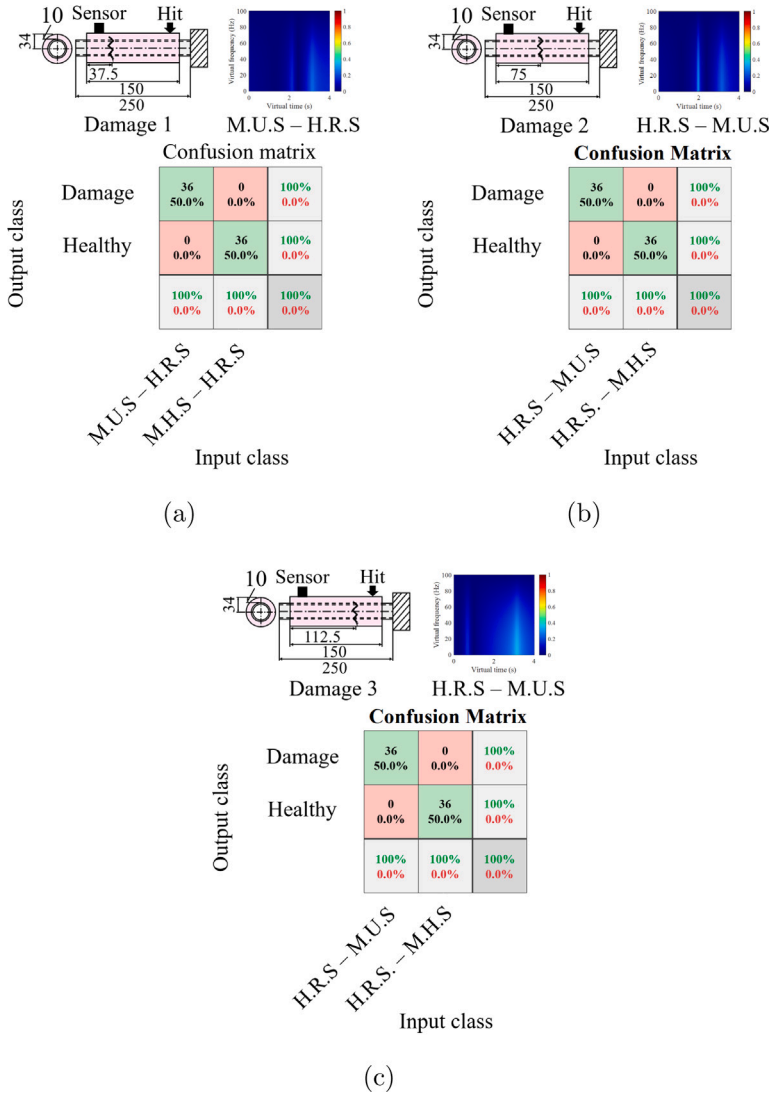

Fig. 8. The confusion matrices of the virtual spectrograms of the differences between the healthy reference signal and the mapped unknown signal (H.R.S-M.U.S) with plastic bar and silicon. The locations of the damages: 37.5 mm in (a), 75 mm in (b) and 112.5 mm in (c).

model is presented and it is assumed that the signal of the damaged real model is not available or not obtainable in priority. The differences among the simplified reference models and the complex real models are the differences in geometry. These assumptions are made to simulate the situation where the signals of the complex real damaged model are not available numerically.

Step 1: Defining the nonlinear transformation function

Fig. 6(a) shows the definition process of the nonlinear transformation function using the responses of the healthy reference model and the healthy complex real model. With the help of the nonlinear transformation function, the healthy signal (H.S.) is transferred to the mapped healthy signal (M.H.S). As illustrated in the right bottom in Fig. 6(a), the curves of H.R.S. and M.H.S show the similarity. Note that the D.R.S. (Damaged Reference Signal) response showing the lower resonance frequency is different to the H.R.S. (Healthy Reference Signal) response. In this first step, the reference models with and without various damages and their responses are considered.

Step 2: Measuring and transformation the unknown signal (U.S.)

Fig. 6(b) shows the process of the measurement of the unknown system, i.e., the system whose condition is not known. The measured signal is then transferred again with the nonlinear transformation function defined in the Step 1 (U.S. (Unknown Signal) ⇒ M.U.S. (Mapped Unknown Signal)). By comparing with the M.U.S. response with the reference signals, i.e., H.R.S. (Healthy Reference Signal) and D.R.S. (Damaged Reference Signal), it is possible to determine that the unknown real system has the similar damage or not. Note that in the present study, it is assumed the responses of the simple reference systems with and without damage

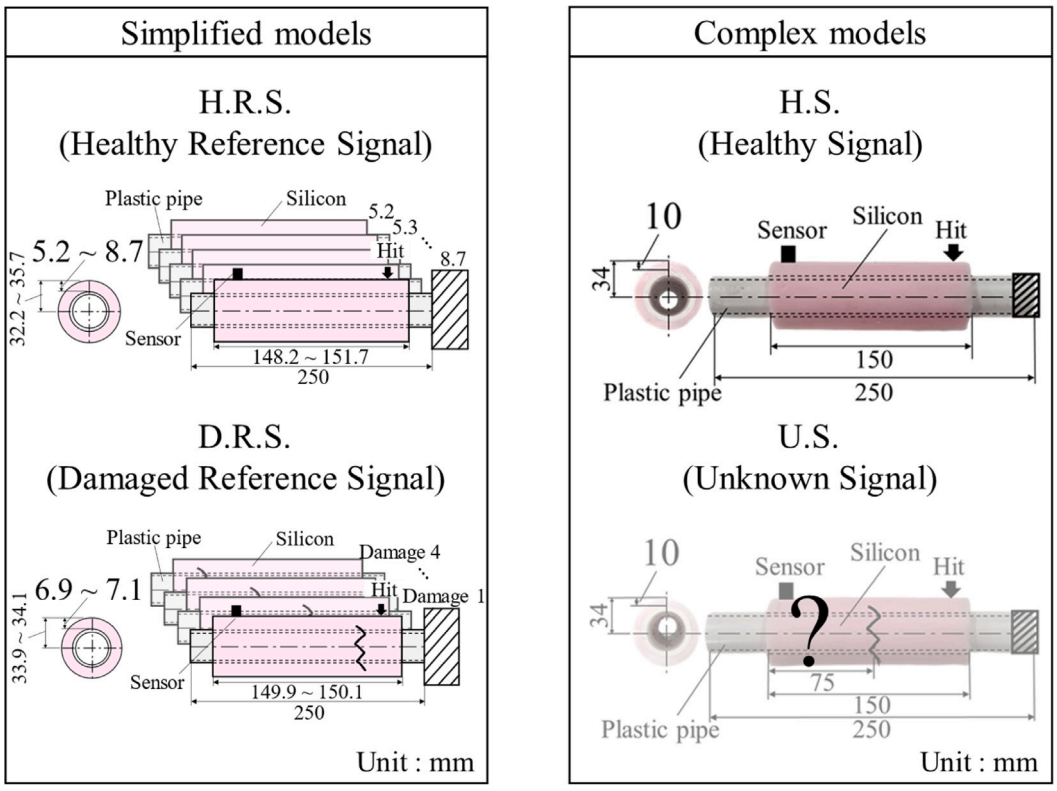

(a)

Fig. 9. Illustration of geometric configurations represented by simplified and complex real models with plastic bar and silicon.

Table 2
The CNN architecture in detail.

Layer name	Layer description
Input	$256 \times 256 \times 3$ Virtual spectrogram image
Convolution 1, Pooling 1	Convolution filter 3 × 3, strides 1, Number of filter = 16, ReLU, Batch normalization, Max pooling filter 2 × 2, strides 2
Convolution 2, Pooling 2	Convolution filter 3 × 3, strides 1, Number of filter = 32, ReLU, Batch normalization, Max pooling filter 2 × 2, strides 2
Convolution 3, Pooling 3	Convolution filter 3 × 3, strides 1, Number of filter = 64, ReLU, Batch normalization, Max pooling filter 2 × 2, strides 2
Convolution 4, Pooling 4	Convolution filter 3 × 3, strides 1, Number of filter = 128, ReLU, Batch normalization, Max pooling filter 2 × 2, strides 2
Convolution 5, Pooling 5	Convolution filter 3 × 3, strides 1, Number of filter = 256, ReLU, Batch normalization, Max pooling filter 2 × 2, strides 2
Convolution 6, Pooling 6	Convolution filter 3 × 3, strides 1, Number of filter = 512, ReLU, Batch normalization, Max pooling filter 2 × 2, strides 2
Fully connected Softmax	Input = 8192, Output = 2048, ReLU Input = 2048, Output = 2

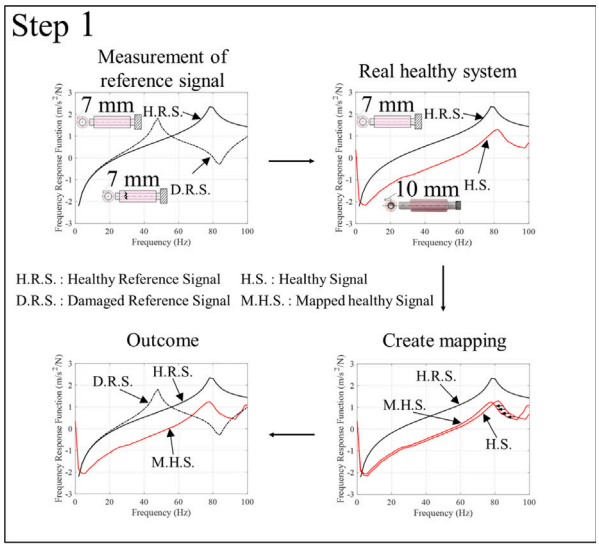

(a)

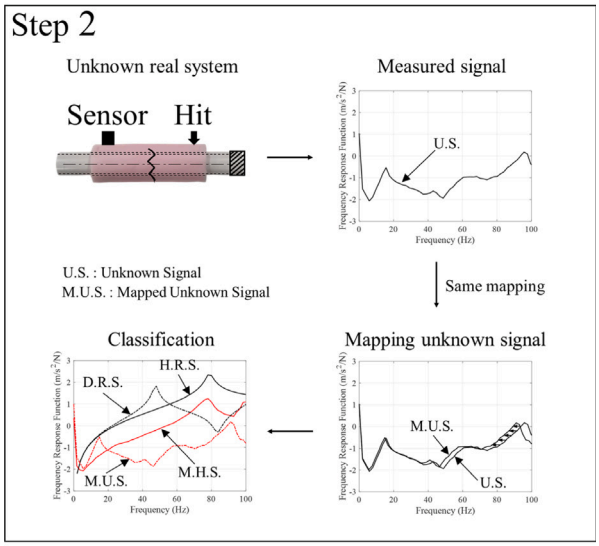

(b)

Fig. 10. The process of nonlinear mapping with real plastic bar and silicon models. (a) Mapping process of reference signals of simplified models and healthy signal of complex real model and (b) mapping process of reference signals of simplified models and unknown signal of complex real models.

can be easily obtained. By making the databases with the simplified reference models and the complex healthy model, we insist that it is possible to obtain the approximate responses of complex damaged systems.

Virtual spectrogram images

After obtaining the data with the nonlinear transformation function, the virtual spectrogram images are generated and utilized as the training and verification data set in Fig. 7(a). Fig. 7(a) shows several representative virtual spectrograms with the difference between the healthy reference signal (H.R.S.) and the mapped healthy signal (M.H.S.) and between the damage reference signal (D.R.S.) and the healthy reference signal (H.R.S.). In this stage, several vertical damages are considered for the damage reference signal.

These images show the distinct differences which can be utilized to train the CNN algorithm. To achieve this purpose, in this first example, we devise 36 healthy simplified finite element models. Without losing generality, the thickness and length are simultaneously changed from 5.2 mm to 8.7 mm and from 148.2 mm to 151.7 mm by a difference of 0.1 mm. Thus, the 36 spectrogram images based on the vibration data of the 36 healthy simple models and 1 healthy real model can be obtained.

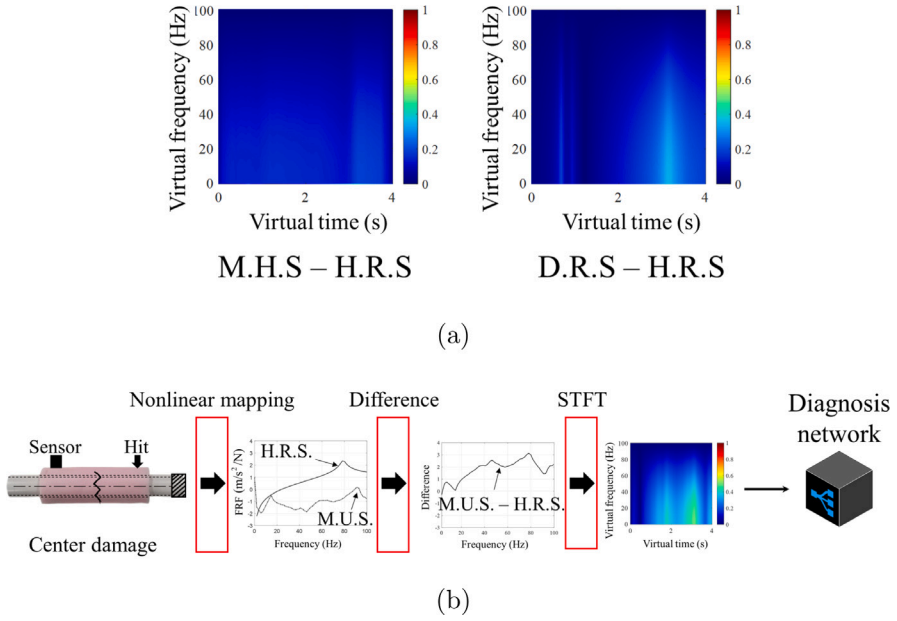

Fig. 11. The virtual spectrograms of the real damages (the locations of the damages at 75 mm). (a) The virtual spectrograms with and without the damage and (b) the virtual spectrogram images of center damages.

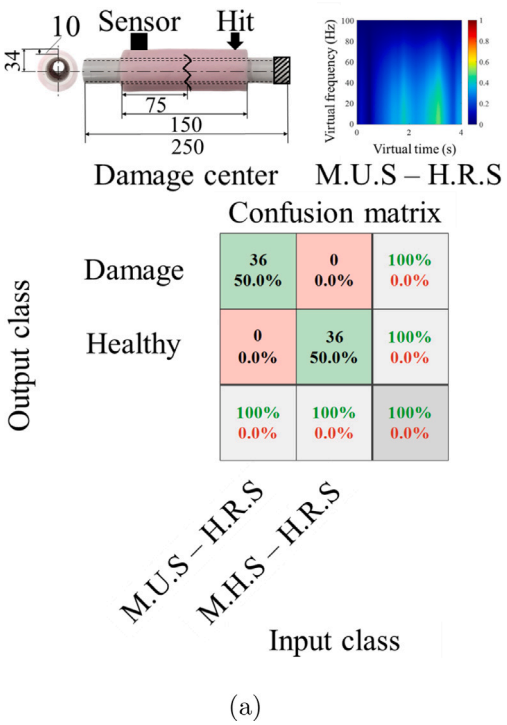

Fig. 12. The confusion matrices of the virtual spectrograms of the differences between the healthy reference signal and the mapped unknown signal (H.R.S - M.U.S) with real plastic bar and silicon. The location of the damage: 75 mm.

With the vibration data of the 36 healthy simple models, the number of the virtual spectrogram images combining the 36 data from H.R.S. (Healthy Reference Signal) with the one M.H.S. (Mapped Healthy Signal), i.e., is 36 (36 × 1). After that, we also consider 12 damaged reference models. The three finite element models with a thickness of 6.9 mm, 7.0 mm and 7.1 mm were selected. Then, the four different cracks are modeled for each of the three models, resulting in a total of 12 models. With the vibration data of the

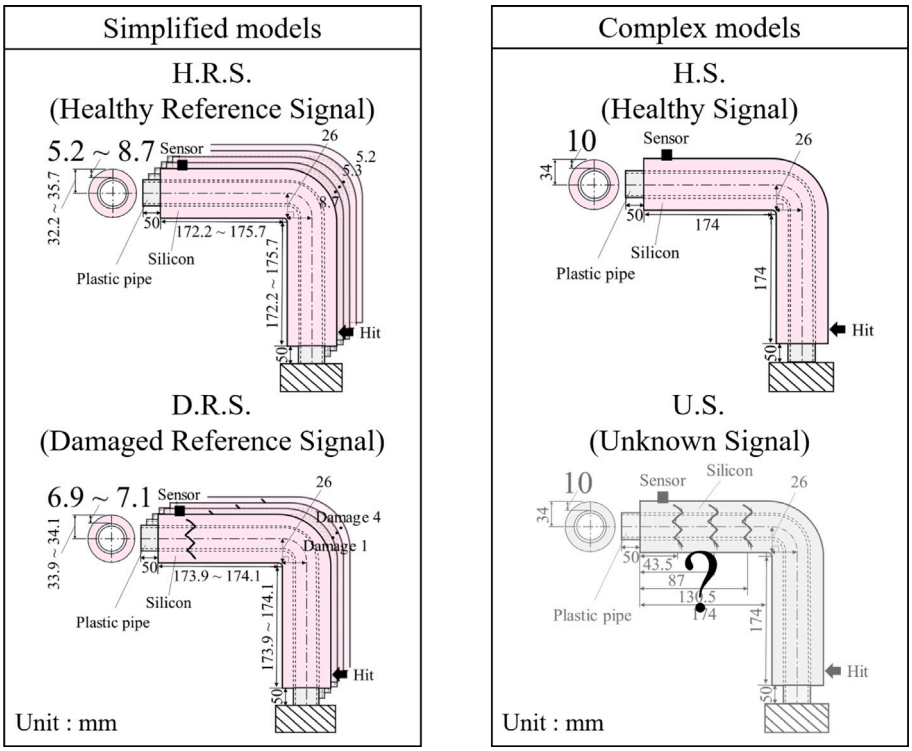

Fig. 13. Illustration of geometric configurations represented by several simplified and complex models with bent plastic bar and silicon (silicon: $\rho = 1500$ kg/m^3, E = 1 MPa, $\nu = 0.47$, bent plastic pipe: $\rho = 1330$ kg/m^3, E = 2 GPa, $\nu = 0.4$).

12 models, the number of the virtual spectrogram images combining the D.R.S. (Damaged Reference Signal) with the three H.R.S. (Healthy Reference Signal), i.e., the model with 6.9 mm, 7.0 mm and 7.1 mm, is also 36 (12 × 3).

Training the deep learning algorithm and classification of unknown signal

The CNN algorithm can be trained and tested with the 72 virtual spectrogram images (36 images from the differences of the 36 healthy reference signals (H.R.S.) and the 1 healthy signal of the healthy real model (H.S.) and 36 images from the differences of the 12 damaged reference signals (D.R.S.) and the 3 healthy reference signal (H.R.S.); it should be emphasized that the signals of the damaged real system are not required for the training data. The training process is carried out with each set of 36 images and the remaining spectrogram images are used to check the validity of the trained network using the confusion matrix. The confusion matrix shows that the training is successful or not.

As the final step, the classifications of several unknown signal (U.S.) is carried out with the present deep learning algorithm in Figs. 7 and 8. The unknown signals in this example are generated with the complex models with the damages at the different locations of the specimen. For example, the three kind of damages in the complex real models are considered in Fig. 7. Then the signals are mapped to the mapped unknown signals (M.U.S.). The difference operator between the M.U.S. and the M.R.S. are calculated. At this stage, the transverse vibration data of the healthy real model can be used. Then the images are generated by the short time Fourier transformation. Fig. 8 shows the confusion matrices of the three signals. As shown it is possible to obtain 100% successful rates. This first example shows the applicability of the present scheme.

In order to verify the present method, the application for real plastic bar and silicon model was presented. To measure the vibration signal, the accelerometer (PCB 352C33) and the impact hammer (PCB 086C03) are employed and the NI-9234 DAQ device is used for the data acquisition. For the simplified models, the finite element simulations are employed in Fig. 9. The real and complex model is the real plastic bar and silicon model in Fig. 9. The frequency response functions of the transverse vibration experiments of these models and the mapping process are illustrated in Fig. 10. To minimize the experimental error, the presented FRFs of the real model using the transverse vibration experiment is obtained by averaging the responses of the ten experiments. It is observed that unlike the finite element simulation, the real experiment has an uneven curve with the damping effect and inconsistent experiment. The eigen modes of the real healthy model and the simulated healthy reference model before the mapping are different. As the result of the nonlinear mapping process, the peak frequencies of H.R.S. and M.H.S. and the slopes become similar. On the other hand, the H.R.S. and M.U.S. are different. Fig. 11 presents a representative virtual spectrogram to be utilized as train and test data. The confusion matrix using the CNN based deep learning algorithm shows the applicability of damage detection of unknown signals with real plastic bar and silicon model in Fig. 12.

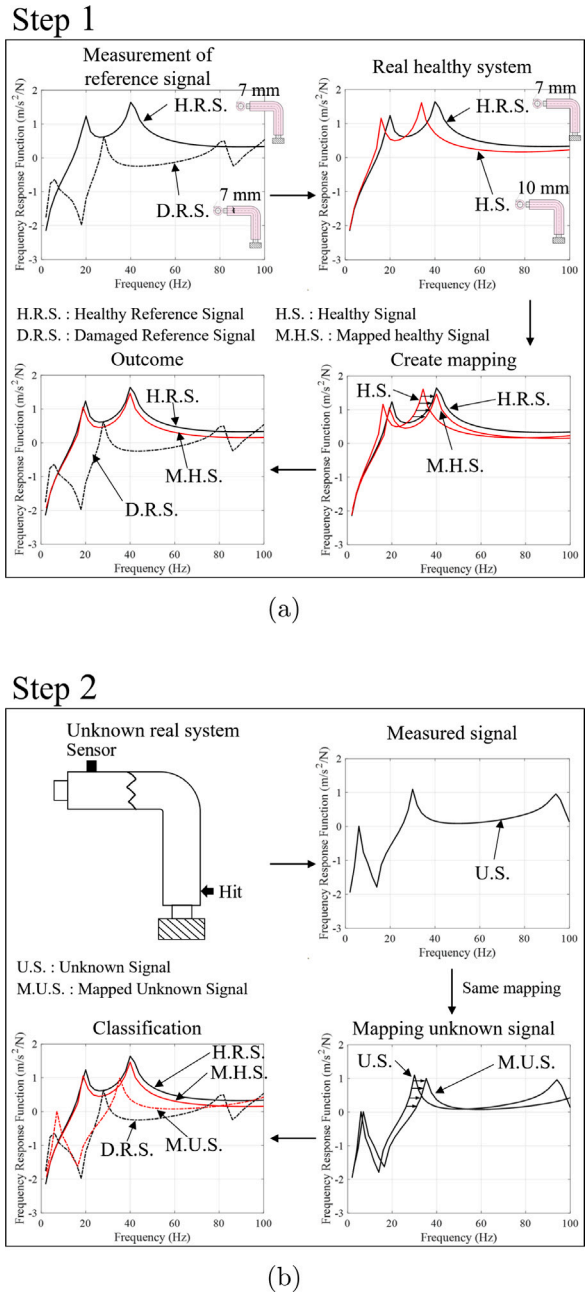

Fig. 14. The process of nonlinear mapping into FRFs with bent plastic bar and silicon models. (a) Mapping process of reference signals of simplified models and healthy signal of complex model and (b) mapping process of reference signals of simplified models and unknown signal of complex models.

4.2. Example 2: The bent plastic bar and silicon models

For the second example, the bent structures in Fig. 13 are considered. The materials of the structures are set to those of PVC plastic for the internal pipe and those of silicon for the coating structure. The impact force is applied at the bottom of the structure and the vibrations are measured at the upper part. As in the first example, the simplified and the real models have the similar geometries. As in the first example, it is assumed that the responses of the healthy reference model and the damaged reference model can be obtained easily. The vibration signal of the healthy model is also obtained easily.

First of all, the vibration signals of the H.R.S. and the H.S. in Fig. 13 are measured and utilized to define the nonlinear transformation function mapping the frequency response function of the real healthy system and the reference system as shown in Fig. 14(a). With the nonlinear transformation function, the vibration data of the real system are transferred from the perspective

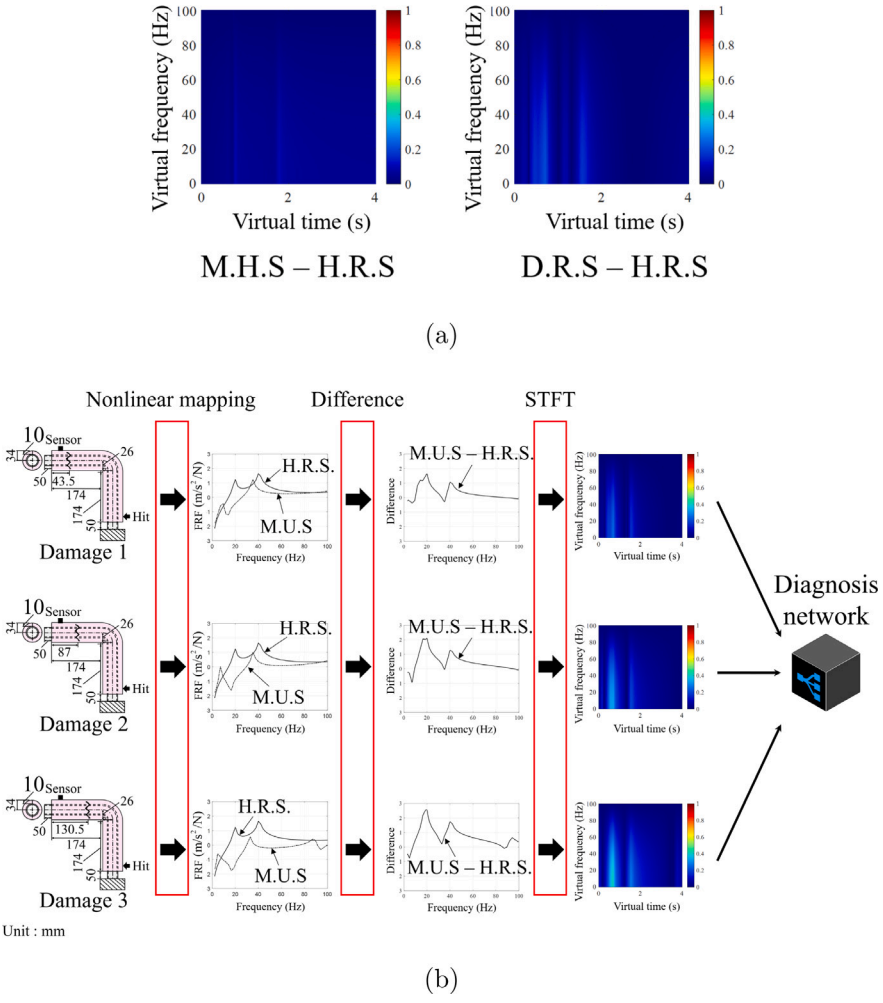

Fig. 15. The virtual spectrograms of the three different damages (the locations of the damages at 43.5 mm, 87 mm and 130.5 mm). (a) The virtual spectrograms with and without the damage and (b) the virtual spectrogram images of various damages.

of the reference model. For the second step, the structural vibration of the unknown real system with damages in Fig. 14(b) is measured. With the same nonlinear transformation function, it also can be transferred from the perspective of the reference model. The mapping unknown signal (M.U.S.) in the bottom right figure in Fig. 14(b) shows the similarity with the vibration data of the damaged reference signal (D.R.S.). Therefore, it can be concluded that the considered unknown real system has the similar crack or fracture. With the help of the CNN based deep learning algorithm trained with the vibration signals of the healthy and damaged reference systems and the healthy real system, it is possible to make the automatic determination process. To do this, the vibration signals of several reference systems with and without damages with the variations of the geometries are measured. The thickness of the healthy model is varied from 5.2 mm to 8.7 mm with 0.1 mm difference and the length is also varied from 385.24 mm to 392.24 mm with 0.2 mm difference in Fig. 13. Thus, the total number of the models is 36. The four different damages of the simplified reference models with the different thickness values, i.e., 6.9 mm, 7.0 mm and 7.1 mm, are considered too. The differences between the healthy reference signals and the mapped healthy signal (H.R.S. - M.H.S.) and the differences between the healthy reference signal and the damaged reference signals (H.R.S. - D.R.S.) are computed and the virtual spectrogram images are generated. Note that in this process to obtain the virtual spectrogram images, the healthy reference systems, the damaged reference system and the healthy real system are required; the vibration signal of the damaged real system is not required. With these virtual spectrogram images, now, it is possible to train the CNN based deep learning algorithm for the automatic classification. After training the deep learning algorithm, the vibration signals of the damaged real systems are obtained and prepared for the input signals of the deep learning algorithm. Figs. 15(b) and 16 shows the results of the this classification process. Fig. 16 shows the confusion matrices of the various cracks located at 43.5 mm, 87 mm and 130.5 mm.

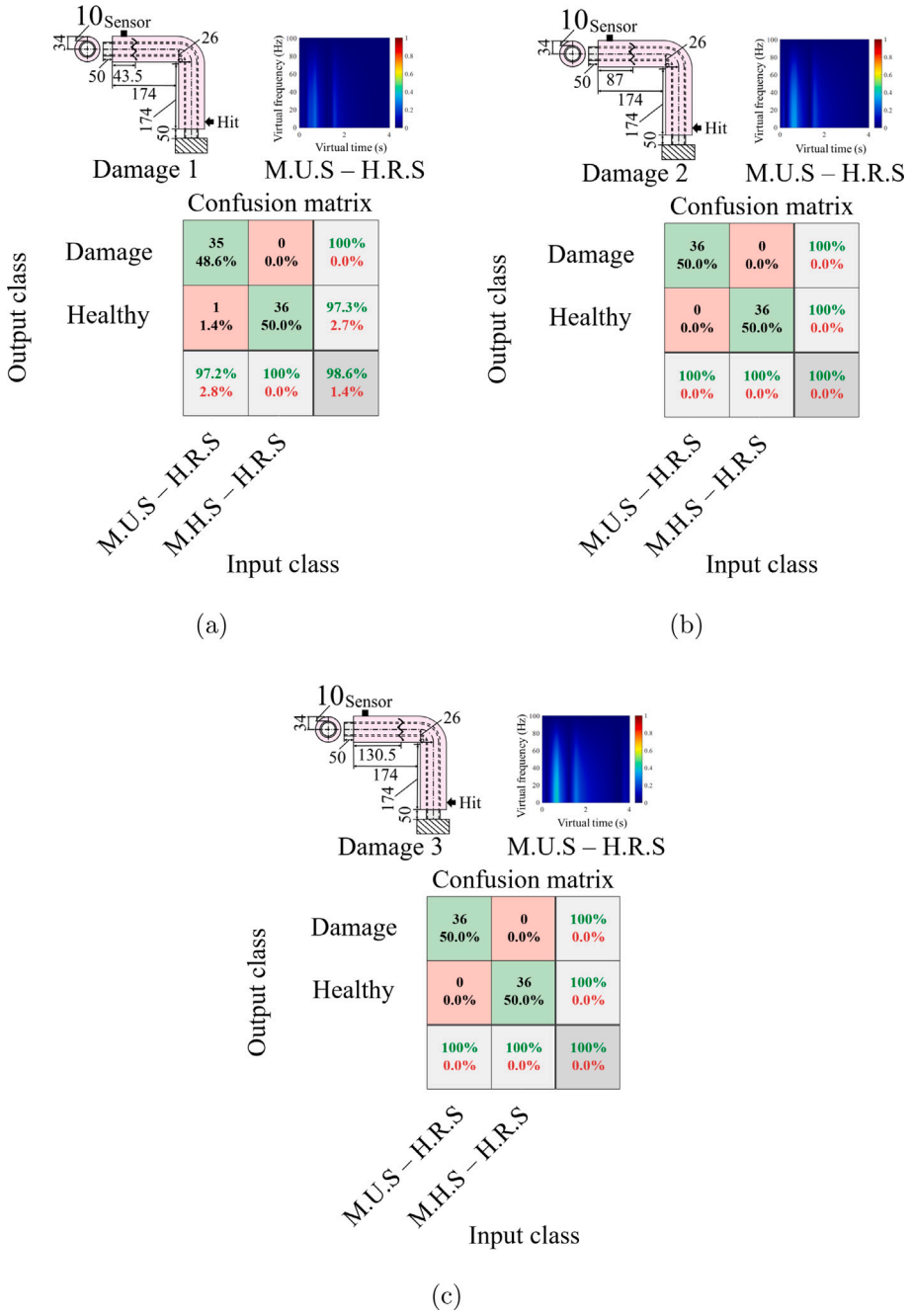

Fig. 16. The confusion matrix of virtual spectrograms of the difference between the healthy reference signal and mapped unknown signal (H.R.S-M.U.S) with bent plastic bar and silicon. The locations of the damages: 43.5 mm in (a), 87 mm in (b) and 130.5 mm in (c).

4.3. Example 3: The mode crossing model

This example describes the process of applying the nonlinear mapping function of the models in which the mode crossing phenomenon occurs. The healthy and damaged simple steel bars in Fig. 17(left) are considered as the reference systems where the PVC composite bar is considered as a complex system in Fig. 17(right). It should be emphasized that the damaged real model is not known in priority however it is assumed that the damage occurs in the middle of the structures. One of the particular characteristics compared with the first two examples lies in the mode switching phenomenon referring that the orders of the eigenmodes are switched among the resonance modes of the reference model and the real model.

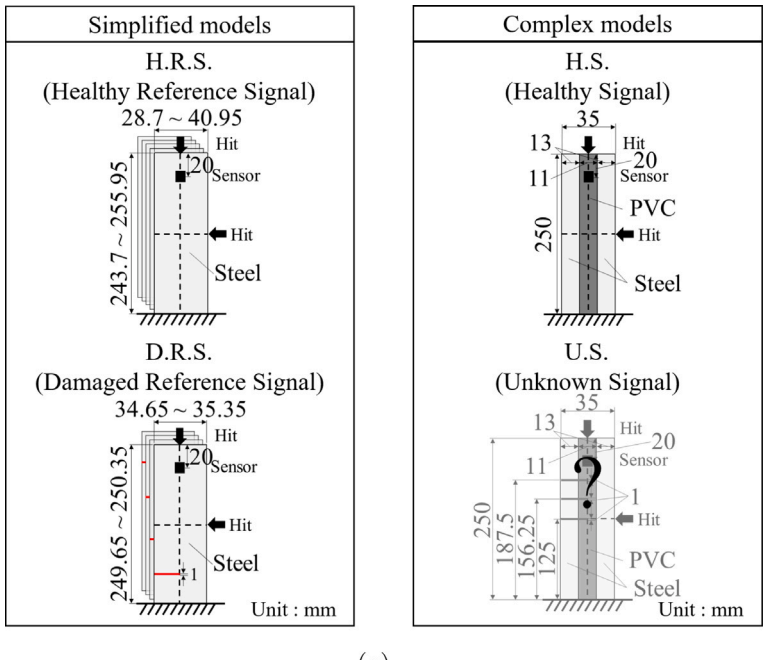

(a)

Fig. 17. Illustration of geometric configurations of simplified and complex models with the mode crossing (steel: $\rho = 7850$ kg/m^3, E = 20 GPa, $\nu = 0.3$, PVC: $\rho = 1390$ kg/m^3, E = 2.86 GPa, $\nu = 0.4$).

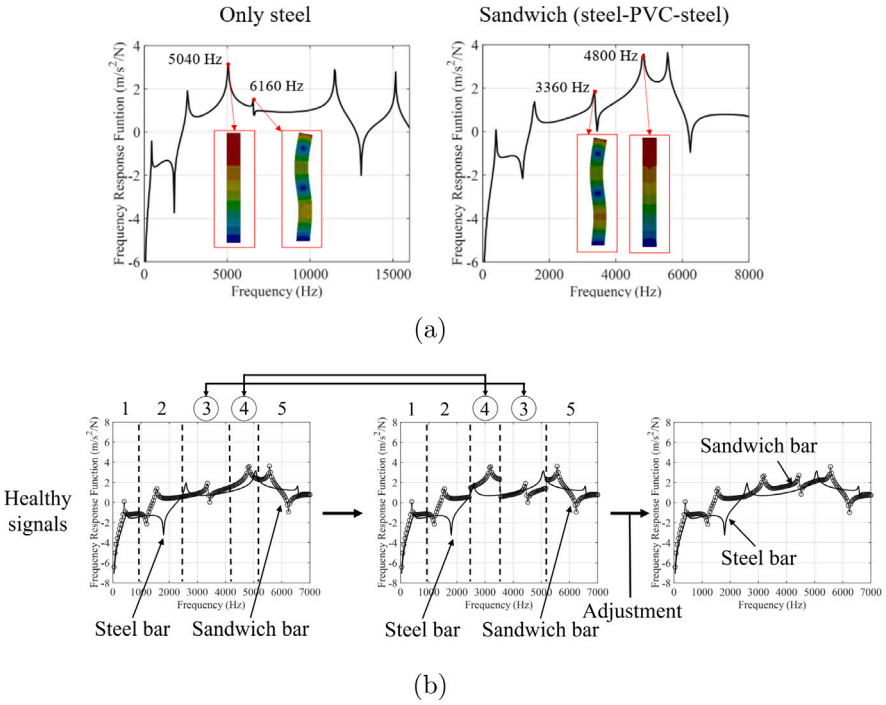

(b)

Fig. 18. The illustration of mode switching. (a) The mode switching between the vibration data of steel bar and composite bar and (b) the adjustment of the vibration data.

Fig. 18(a) shows the vibration data of the simplified reference model and the complex real model. From this graph, it is found that the third mode and the fourth mode of the reference model and the real composite models are the extension mode and the higher bending mode, but they are switched. To reflect the effect of the mode cross in the structural vibration, the middle lines

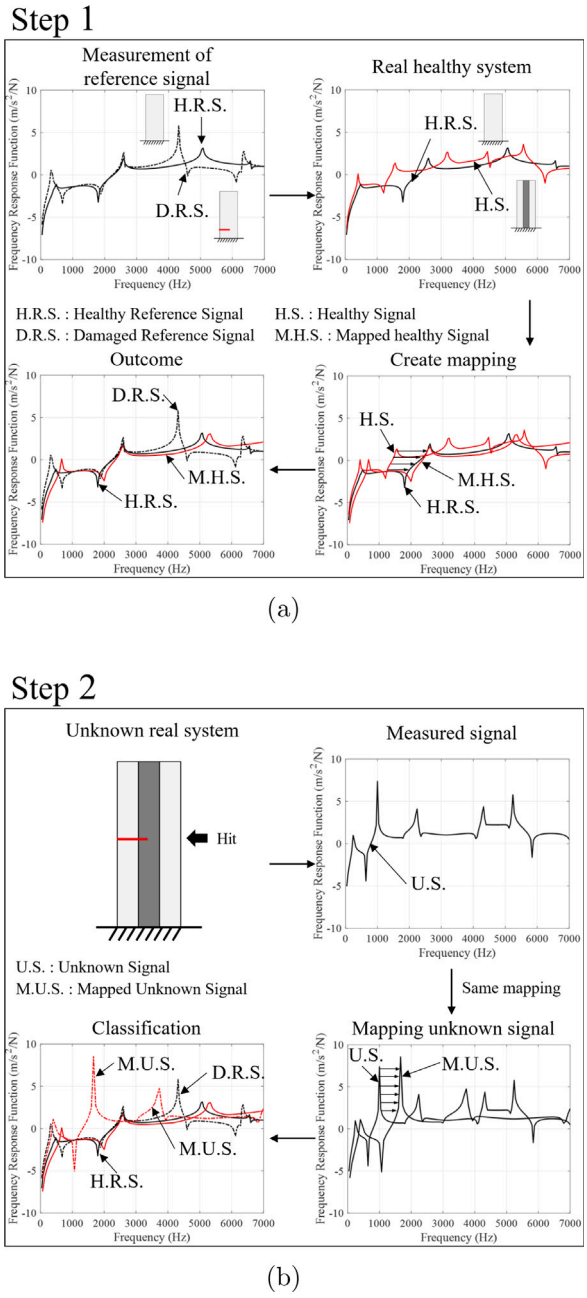

Fig. 19. The process of nonlinear mapping into FRFs with mode crossing models. (a) Mapping process of reference signals of simplified models and healthy signal of complex model and (b) mapping process of reference signals of simplified models and unknown signal of complex models.

among the resonance peaks are calculated in Fig. 18(b) (marked as the dotted lines in Fig. 18(b)). Then the sections marked by 3 and 4 are switched to consider the mode switching phenomenon. After this operation, some discontinuous points are observed at the intersection lines between the second domain and the fourth domain and between the third domain and the fifth domain. Therefore, the additional operations making snitching the discontinuous curves are applied. For example, the first point of the fourth domain is offset to meet the end point of the second section. Then the first point of the third section is offset to meet the end point of the fourth section. Finally, the first point of the fifth domain is offset to meet the end point of the third section as illustrated in Fig. 18(b).

After this procedure, with the structural vibration data of the healthy steel bar and the healthy sandwich bar, the nonlinear mapping is defined as shown in Fig. 19(a). At the second step, the damaged real system is now diagnosed in Fig. 19(b). To account the mode switching, the operation explained in Fig. 18(b) is applied to the vibration data of the damaged real model as shown in

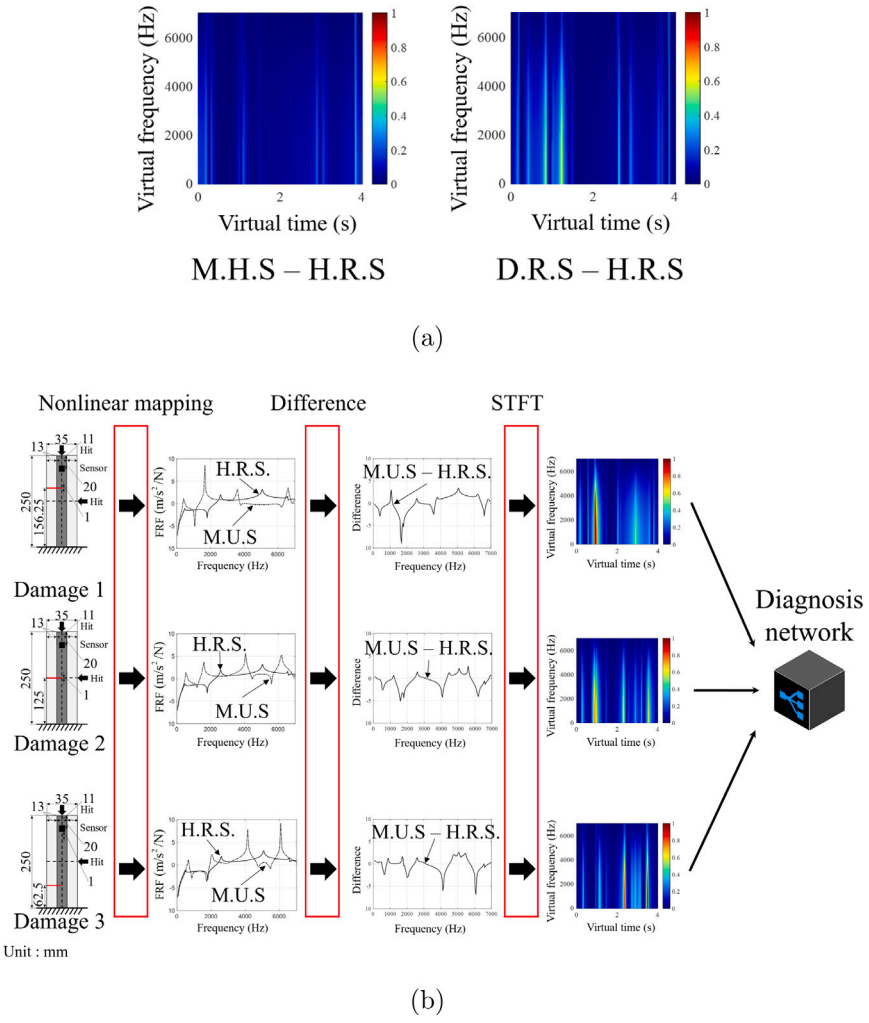

Fig. 20. The virtual spectrograms of the three different damages (the locations of the damages at 62.5 mm, 125 mm and 156.25 mm). (a) The virtual spectrograms with and without the damage and (b) the virtual spectrogram images of various damages.

Fig. 19(b). Then the nonlinear transformation function defined in Fig. 18(a) is applied to that signal in order to identify whether the measured signal is came from a damaged real model or a healthy real model.

With several simulation data similar to the previous example, the virtual spectrogram images can be computed in Fig. 20(a). These images are used to make a CNN network for the diagnosis system. Fig. 20(b) shows a series of examples with the various damages of the real system and their virtual spectrogram images. The trained CNN algorithm shows the accuracy in Fig. 21. Finally this example illustrates the application of the present diagnosis example with a real model with the mode switching phenomenon.

5. Conclusion

This study addresses the application of the nonlinear transformation-based augmentation method with vibration signals of simple, small scale and elementary models for Convolutional Neural Network (CNN) approach for the classification and prediction of perplex healthy or damaged systems using a smart diagnosis system. For the accuracy classification with the machine learning algorithm, sufficient data should be provided for the training process. Many engineering applications domains in mechanical or civil engineering allow to provide data in healthy condition of systems of interest but do not allow data in not-healthy or damaged condition. To compensate this deficiency, the present study suggests to utilize the data from healthy and damaged small scale elementary models. With the vibration data from the healthy elementary model and the healthy real model, the nonlinear transformation function is defined first. This defined nonlinear transformation function is then applied to argument the vibration data from the damaged small scale models to predict the approximate vibration data from damaged real models. These data sets are utilized to train the deep learning algorithm for the classification. In order to illustrate the applications of this data argumentation approach, the classifications of several vibration examples are considered. With the example with the mode switching model, the nonlinear transformation

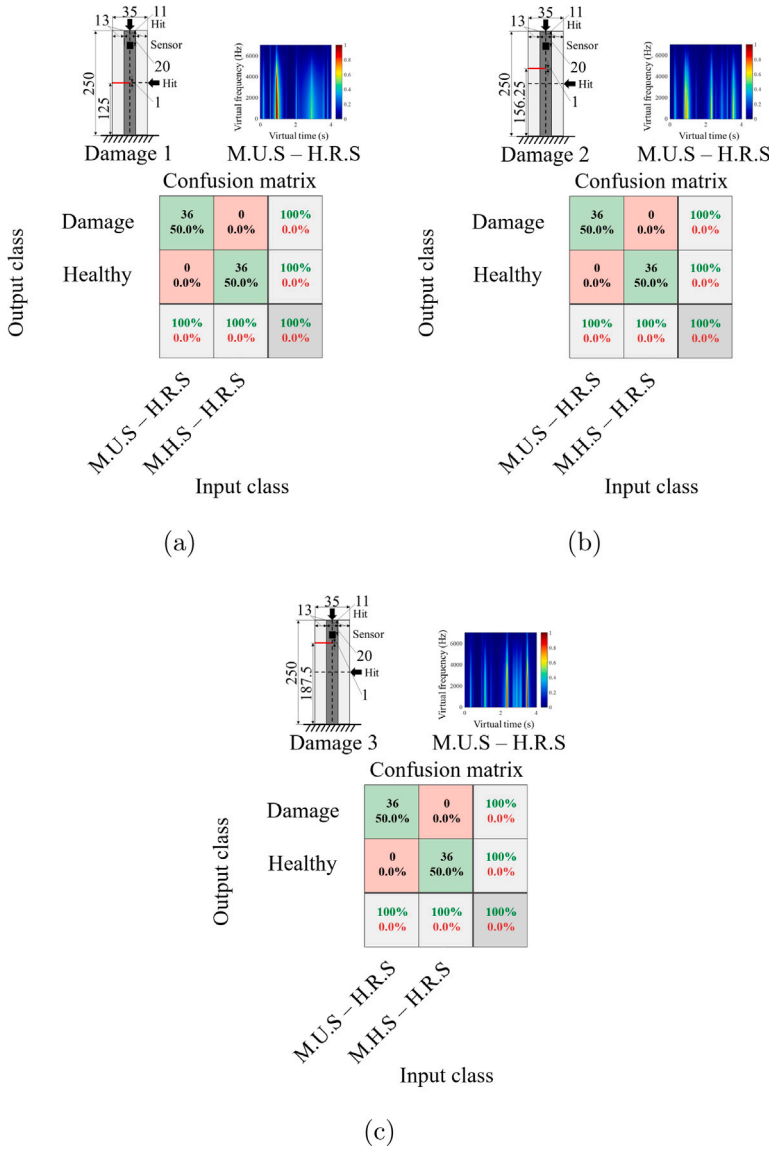

Fig. 21. The confusion matrix of the virtual spectrograms of the difference between the healthy reference signal and mapped unknown signal (H.R.S-M.U.S) with mode crossing models. The locations of the damages: 125 mm in (a), 156.25 mm in (b) and 187.5 mm in (c).

function considering the mode switching phenomenon is developed and applied. The confusion matrix shows that the prediction accuracy is high. The accuracy of the CNN trained with the augmented data with the present nonlinear mapping is over 98% for the two vibration models with and without the mode switching phenomenon. One of the limitations of the presented method is that it will be intricated to identify damage with the small difference between the healthy reference signal and the damage reference signal, large damping, or new random eigenmodes after damage in the frequency domain. For future research, the present nonlinear mapping method should be verified with various applications.

Declaration of competing interest

The authors declare that they have no known competing financial interests or personal relationships that could have appeared to influence the work reported in this paper.

Acknowledgment

The authors are grateful for the financial support received from the National Research Foundation (NRF) of Korea grant funded by the Korea government (MSIT) (NRF-2019R1A2C2084974).

References

[1] C. Shorten, T.M. Khoshgoftaar, A survey on image data augmentation for deep learning, J. Big Data 6 (1) (2019) 1–48.
[2] J. Wang, L. Perez, et al., The effectiveness of data augmentation in image classification using deep learning, Convolutional Neural Netw. Vis. Recognit. 11 (2017).
[3] E.D. Cubuk, B. Zoph, D. Mane, V. Vasudevan, Q.V. Le, Autoaugment: Learning augmentation strategies from data, in: Proceedings of the IEEE/CVF Conference on Computer Vision and Pattern Recognition, 2019, pp. 113–123.
[4] J.A. Royle, R.M. Dorazio, W.A. Link, Analysis of multinomial models with unknown index using data augmentation, J. Comput. Graph. Statist. 16 (1) (2007) 67–85.
[5] A. Khan, D.-K. Ko, S.C. Lim, H.S. Kim, Structural vibration-based classification and prediction of delamination in smart composite laminates using deep learning neural network, Composites B 161 (2019) 586–594.
[6] A. Khan, J.K. Shin, W.C. Lim, N.Y. Kim, H.S. Kim, A deep learning framework for vibration-based assessment of delamination in smart composite laminates, Sensors 20 (8) (2020) 2335.
[7] L. Chen, Z. Zhang, J. Cao, A novel method of combining generalized frequency response function and convolutional neural network for complex system fault diagnosis, PLoS One 15 (2) (2020) e0228324.
[8] W. Zhang, G. Peng, C. Li, Y. Chen, Z. Zhang, A new deep learning model for fault diagnosis with good anti-noise and domain adaptation ability on raw vibration signals, Sensors 17 (2) (2017) 425.
[9] S. Boschert, R. Rosen, Digital twin—the simulation aspect, in: Mechatronic Futures, Springer, 2016, pp. 59–74.
[10] J. Wang, L. Ye, R.X. Gao, C. Li, L. Zhang, Digital twin for rotating machinery fault diagnosis in smart manufacturing, Int. J. Prod. Res. 57 (12) (2019) 3920–3934.
[11] P. Jain, J. Poon, J.P. Singh, C. Spanos, S.R. Sanders, S.K. Panda, A digital twin approach for fault diagnosis in distributed photovoltaic systems, IEEE Trans. Power Electron. 35 (1) (2019) 940–956.
[12] A. Kumar, C. Gandhi, Y. Zhou, G. Vashishtha, R. Kumar, J. Xiang, Improved cnn for the diagnosis of engine defects of 2-wheeler vehicle using wavelet synchro-squeezed transform (wsst), Knowl.-Based Syst. 208 (2020) 106453.
[13] Y.-M. Hsueh, V.R. Ittangihal, W.-B. Wu, H.-C. Chang, C.-C. Kuo, Fault diagnosis system for induction motors by cnn using empirical wavelet transform, Symmetry 11 (10) (2019) 1212.
[14] M. Sohaib, J.-M. Kim, Fault diagnosis of rotary machine bearings under inconsistent working conditions, IEEE Trans. Instrum. Meas. 69 (6) (2019) 3334–3347.
[15] F. Nex, D. Duarte, F.G. Tonolo, N. Kerle, Structural building damage detection with deep learning: Assessment of a state-of-the-art cnn in operational conditions, Remote Sens. 11 (23) (2019) 2765.
[16] J.D. Poston, J. Schloemann, R.M. Buehrer, V.S. Malladi, A.G. Woolard, P.A. Tarazaga, Towards indoor localization of pedestrians via smart building vibration sensing, in: 2015 International Conference on Localization and GNSS (ICL-GNSS), IEEE, 2015, pp. 1–6.
[17] Z. Wang, N. Yang, N. Li, W. Du, J. Wang, A new fault diagnosis method based on adaptive spectrum mode extraction, Struct. Health Monit. (2021) 1475921720986945.
[18] S.-Y. Li, K.-R. Gu, S.-C. Huang, A chaotic system-based signal identification technology: Fault-diagnosis of industrial bearing system, Measurement 171 (2021) 108832.
[19] Y. Han, W. Qi, N. Ding, Z. Geng, Short-time wavelet entropy integrating improved lstm for fault diagnosis of modular multilevel converter, IEEE Trans. Cybern. (2021).
[20] M. Paszyński, R. Grzeszczuk, D. Pardo, L. Demkowicz, Deep learning driven self-adaptive hp finite element method, in: International Conference on Computational Science, Springer, 2021, pp. 114–121.
[21] A. Hürkamp, S. Gellrich, T. Ossowski, J. Beuscher, S. Thiede, C. Herrmann, K. Dröder, Combining simulation and machine learning as digital twin for the manufacturing of overmolded thermoplastic composites, J. Manufact. Mater. Proces. 4 (3) (2020) 92.
[22] P. Kathirvel, M.S. Manikandan, S. Prasanna, K. Soman, An efficient r-peak detection based on new nonlinear transformation and first-order gaussian differentiator, Cardiovasc. Eng. Technol. 2 (4) (2011) 408–425.
[23] P. Maragos, Slope transforms: theory and application to nonlinear signal processing, IEEE Trans. Signal Process. 43 (4) (1995) 864–877.
[24] Y.-T. Cheng, C.-M. Cheng, Scaling, dimensional analysis, and indentation measurements, Mater. Sci. Eng. R 44 (4–5) (2004) 91–149.
[25] G. Astarita, Dimensional analysis, scaling, and orders of magnitude, Chem. Eng. Sci. 52 (24) (1997) 4681–4698.
[26] K. Weiss, T.M. Khoshgoftaar, D. Wang, A survey of transfer learning, J. Big Data 3 (1) (2016) 1–40.
[27] R. Barman, S. Deshpande, S. Agarwal, U. Inamdar, M. Devare, A. Patil, Transfer learning for small dataset, in: Proceedings of the National Conference on Machine Learning, Mumbai, India, Vol. 26, 2019.
[28] S. Goswami, C. Anitescu, S. Chakraborty, T. Rabczuk, Transfer learning enhanced physics informed neural network for phase-field modeling of fracture, Theor. Appl. Fract. Mech. 106 (2020) 102447.
[29] A. Kamilaris, F.X. Prenafeta-Boldú, Deep learning in agriculture: A survey, Comput. Electron. Agric. 147 (2018) 70–90.
[30] S. Haidong, J. Hongkai, L. Xingqiu, W. Shuaipeng, Intelligent fault diagnosis of rolling bearing using deep wavelet auto-encoder with extreme learning machine, Knowl.-Based Syst. 140 (2018) 1–14.
[31] Z. Chen, T. Zhang, C. Ouyang, End-to-end airplane detection using transfer learning in remote sensing images, Remote Sens. 10 (1) (2018) 139.
[32] Z. Shen, X. Wan, F. Ye, X. Guan, S. Liu, Deep learning based framework for automatic damage detection in aircraft engine borescope inspection, in: 2019 International Conference on Computing, Networking and Communications (ICNC), IEEE, 2019, pp. 1005–1010.
[33] Y. Gong, H. Shao, J. Luo, Z. Li, A deep transfer learning model for inclusion defect detection of aeronautics composite materials, Compos. Struct. 252 (2020) 112681.
[34] G. Liang, L. Zheng, A transfer learning method with deep residual network for pediatric pneumonia diagnosis, Comput. Methods Programs Biomed. 187 (2020) 104964.
[35] J. Krois, T. Ekert, L. Meinhold, T. Golla, B. Kharbot, A. Wittemeier, C. Dörfer, F. Schwendicke, Deep learning for the radiographic detection of periodontal bone loss, Sci. Rep. 9 (1) (2019) 1–6.
[36] R. Yamashita, M. Nishio, R.K.G. Do, K. Togashi, Convolutional neural networks: an overview and application in radiology, Insights Imaging 9 (4) (2018) 611–629.
[37] J. Qin, W. Pan, X. Xiang, Y. Tan, G. Hou, A biological image classification method based on improved cnn, Ecol. Inform. 58 (2020) 101093.
[38] R. Chauhan, K.K. Ghanshala, R. Joshi, Convolutional neural network (cnn) for image detection and recognition, in: 2018 First International Conference on Secure Cyber Computing and Communication (ICSCCC), IEEE, 2018, pp. 278–282.
[39] N. Ketkar, Convolutional neural networks, in: Deep Learning with Python, Springer, 2017, pp. 63–78.
[40] S. Albawi, T.A. Mohammed, S. Al-Zawi, Understanding of a convolutional neural network, in: 2017 International Conference on Engineering and Technology (ICET), Ieee, 2017, pp. 1–6.
[41] P. Kim, Convolutional neural network, in: MATLAB Deep Learning, Springer, 2017, pp. 121–147.
[42] A.F. Agarap, Deep learning using rectified linear units (relu), 2018, arXiv preprint arXiv:1803.08375.

[43] H.H. Aghdam, E.J. Heravi, Guide to Convolutional Neural Networks: A Practical Application to Traffic-Sign Detection and Classification, Springer, New York, NY, 2017.
[44] G.H. Yoon, Y.-J. Woo, S.-G. Sim, D.-Y. Kim, S.J. Hwang, Investigation of bone fracture diagnosis system using transverse vibration response, Proc. Inst. Mech. Eng. Part H (2021) 0954411921997575.
[45] MATLAB, Deep Learning Toolbox Version 14.0 (R2020a), The MathWorks Inc., Natick, Massachusetts, 2020.
[46] E. Balmes, High modal density, curve veering, localization: a different perspective on the structural response, J. Sound Vib. 161 (2) (1993) 358–363.
[47] A. Gallina, L. Pichler, T. Uhl, Enhanced meta-modelling technique for analysis of mode crossing, mode veering and mode coalescence in structural dynamics, Mech. Syst. Signal Process. 25 (7) (2011) 2297–2312.